Proceedings of the SEM Annual Conference
June 7-10, 2010 Indianapolis, Indiana USA

Characterization of Polymeric Foams under Multi-Axial Static and Dynamic Loading

Isaac M. Daniel and Jeong-Min Cho

Robert R. McCormick School of Engineering and Applied Science
Northwestern University
Evanston, IL 60208
imdaniel@northwestern.edu

ABSTRACT

An orthotropic polymeric foam with transverse isotropy (Divinycell H250) used in composite sandwich structures was characterized under multi-axial quasi-static and dynamic loading. Quasi-static tests were conducted along principal material axes as well as along off-axis directions under tension, compression, and shear. An optimum specimen aspect ratio of 10 was selected based on finite element analysis. Stress-controlled and strain-controlled experiments were conducted. The former yielded engineering material constants such as Young's and shear moduli and Poisson's ratios; the latter yielded mathematical stiffness constants, i. e., C_{ij} . Intermediate strain rate tests were conducted in a servo-hydraulic machine. High strain rate tests were conducted using a split Hopkinson Pressure Bar system built for the purpose. This SHPB system was made of polymeric (polycarbonate) bars. The polycarbonate material has an impedance that is closer to that of foam than metals. The system was analyzed and calibrated to account for the viscoelastic response of its bars. Material properties of the foam were obtained at three strain rates, quasi-static (10^{-4} s^{-1}), intermediate (1 s^{-1}), and high (10^{3} s^{-1}) strain rates.

Introduction

A great deal of work is being reported by other investigators dealing with analysis and simulation of impact and blast loading of composite and sandwich structures. The usefulness of the results obtained depends on the type of inputs used for loading pulses and material behavior. Loading pulse information may be obtained from the literature, however, no realistic models are available for the facesheet and core materials under multi-axial dynamic loading, especially models including hygrothermal effects of long term environmental exposure. Characterization and modeling of facesheet composite materials is being addressed and reported in many sources. However, not enough work has been devoted to characterization and constitutive modeling of structural foams used in sandwich construction. Such work is needed to develop numerical models capable of capturing the dynamic response of composite and sandwich structures under realistic impact and blast loadings and design novel structures for mitigation of severe threats.

Cellular foams are commonly used as core materials in sandwich structures. They are usually made of polyvinyl chloride (PVC), polyurethane (PUR) and polystyrene. The properties of foams depend on the structure of the cells and the density of the material. The mechanical behavior of cellular foams has been investigated and discussed in the literature [1-5]. A thorough discussion of mechanical behavior of polymeric foams is given in the book by Gibson and Ashby [1]. However, characterization has been in general inadequate, and few of the models can capture all the characteristic features of structural foams. Sandwich foam core materials, such as PVC foams (especially higher density ones), are strain rate dependent anisotropic elastic/viscoplastic materials. Their deformation history during dynamic loading affects critically the integrity of the sandwich structure. A few studies have been reported on dynamic characterization of foams [6-9]. Constitutive modeling has lagged because of the finite deformations and the anisotropy involved in some foams, with few works reported in the literature [10-12]. Gielen [12] developed a constitutive model including elastic-plastic behavior and damage progression. However, the

T. Proulx (ed.), *Dynamic Behavior of Materials, Volume 1*, Conference Proceedings of the Society for Experimental Mechanics Series,
DOI 10.1007/978-1-4419-8228-5_18, © The Society for Experimental Mechanics, Inc. 2011

model is not easily applicable in analyses. Considering the loading-unloading-reloading test results in [4], a realistic modeling approach is needed based on an elastic-plastic-damage formulation in strain space.

The present paper extends the multi-axial characterization of an anisotropic foam by means of off-axis testing and stress-controlled and strain-controlled experiments. Rate effects were also studied by using a Hopkinson bar system with impedance-matched polymeric rods.

Experimental Procedures

The material studied was a closed cell PVC foam, Divinycell H250, having a density of 250 kg/m^3. The material was obtained in the form of 25 mm thick panels. It is an orthotropic/transversely isotropic material with principal axes as shown in Fig. 1. This material has been characterized before under loading along the principal material axes as shown in Fig.2.

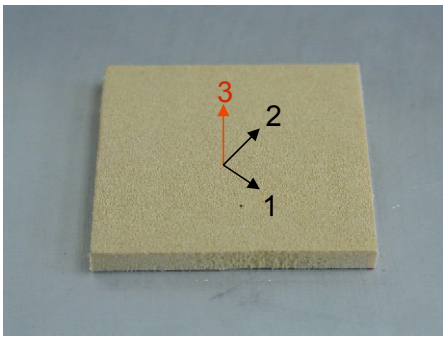

Figure 1. Principal material axes of Divinycell H250 foam

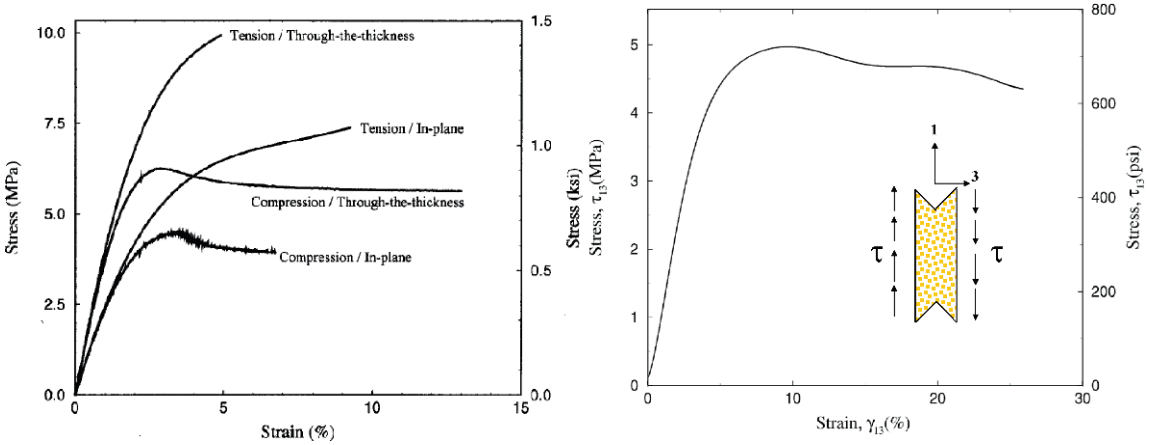

Figure 2. Typical stress-strain curves of Divinycell H250 foam loade along principal directions[2].

A more complete characterization of this material was performed by means of static and high rate tests along principal material axes as well as off-axis directions under tension, compression, and shear (at orientations of 0, 20, 45, 70, and 90 deg with the 3-axis, Fig. 3).

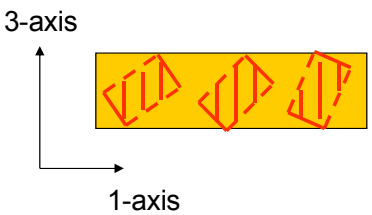

Figure 3. Off-axis testing of foam specimens

On-axis and off-axis coupons were tested under stress control as shown in Fig. 4. Strains were measured by means of Moiré gratings photoprinted on the specimen surface.

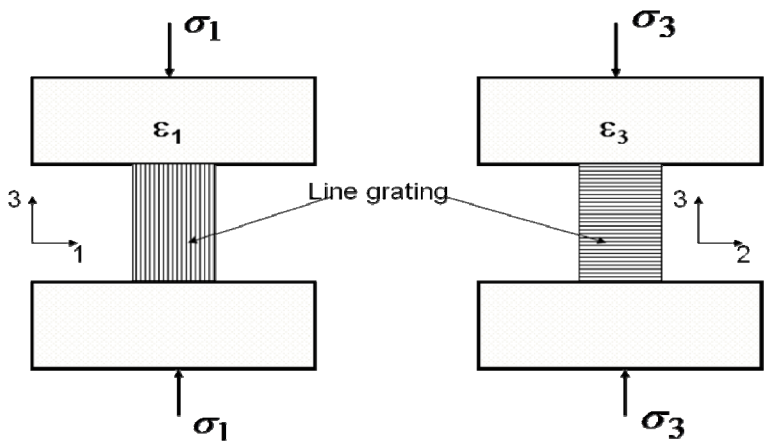

Figure 4. Stress-controlled experiments

Strain-controlled experiments were conducted using specimens and fixtures such as those shown in Fig. 5 at quasi-static and moderate strain rates. These tests, corresponding to strain rates of 10^{-4} and 1 s^{-1}, respectively, were conducted in a servo-hydraulic machine. The optimum specimen aspect ratio was determined by Finite Element Analysis (Fig. 6). The higher the aspect ratio the more homogeneous is the state of strain. An aspect ratio of 10 was deemed suitable for the experiments.

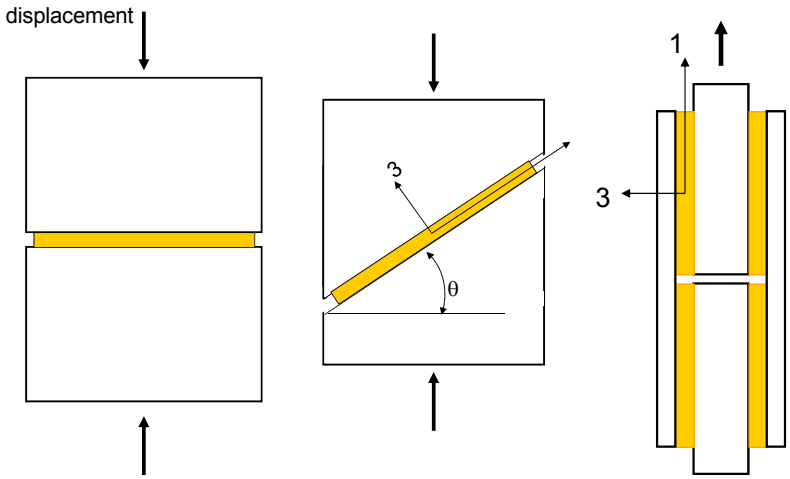

Figure 5. Strain-controlled experiments.

High strain rate tests were conducted using a split Hopkinson Pressure Bar (SHPB) system built for the purpose (Fig. 5). This SHPB system was made of polymeric (polycarbonate) bars. The polycarbonate material has an impedance that is closer to that of foam than metals as shown in Table 1 below. The viscoelastic wave propagation in the polycarbonate rods was analyzed by FFT and the frequency dependence of the attenuation and phase velocity in the rods was determined. The transformed strain, velocity and force (stress) in the specimen were obtained as a function of frequency.

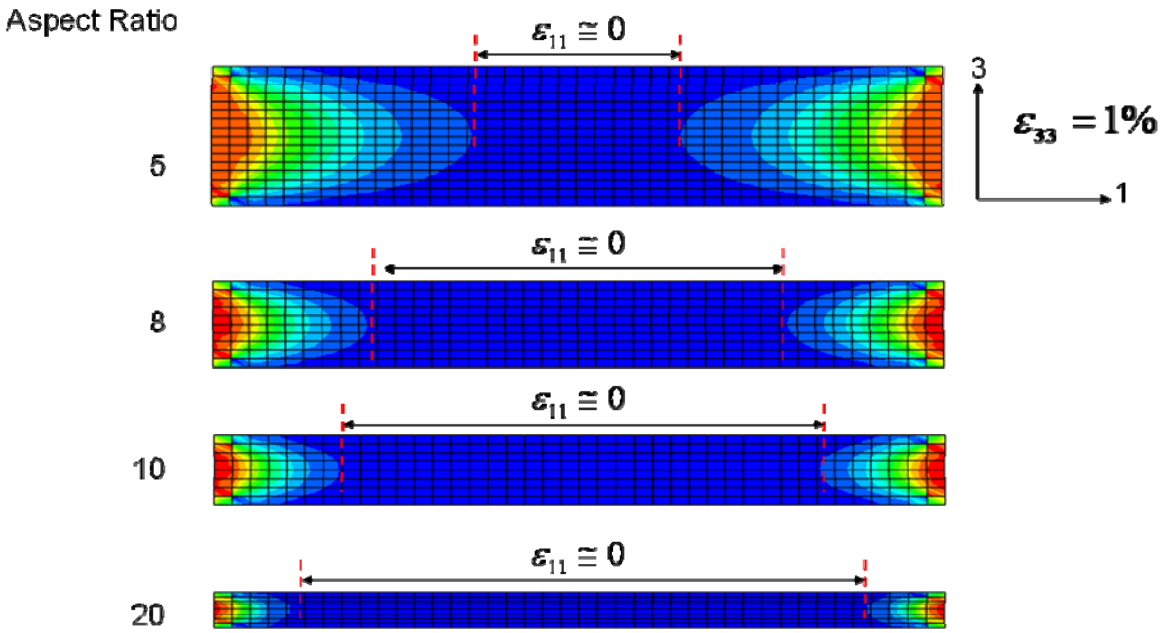

Figure 6. Selection of specimen aspect ratio for strain-controlled experiments

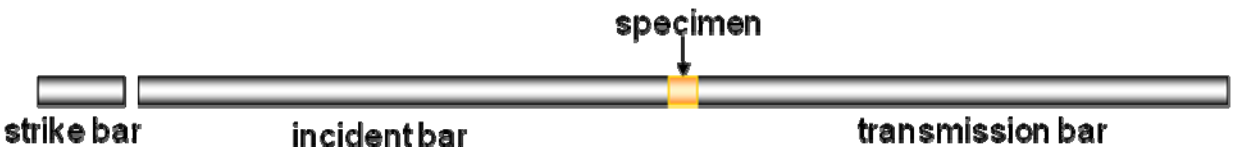

Figure 7. Split Hopkinson pressure bar with polymeric bars for testing foam materials

Table 1. Impedances of Hopkinson bar and foam materials

Material	*E*, MPa	ρ, kg/m^3	$Z(=\rho c)$, kg/m^{2}s
Steel	207,000	7,800	4.0×10^7
Aluminum	73,000	2,800	1.4×10^7
Polycarbonate	2,410	1,200	1.7×10^6
PVC Foam (DIAB H250)	322 (through-thickness)	250	2.8×10^5
PVC Foam (DIAB H250)	207 (in-plane)	250	2.3×10^5

Stress-Controlled Experiments

Compressive stress-strain curves for the off-axis specimens tested under stress-controlled conditions are shown in Fig. 8. The effect of anisotropy and stress biaxiality is reflected in the variation in axial modulus and characteristic first peak in the stress-strain curve. The latter is the “critical point” of initiation of local collapse of the cell structure. The variation of the axial modulus and this critical point with load orientation is shown in Figs. 9 and 10.

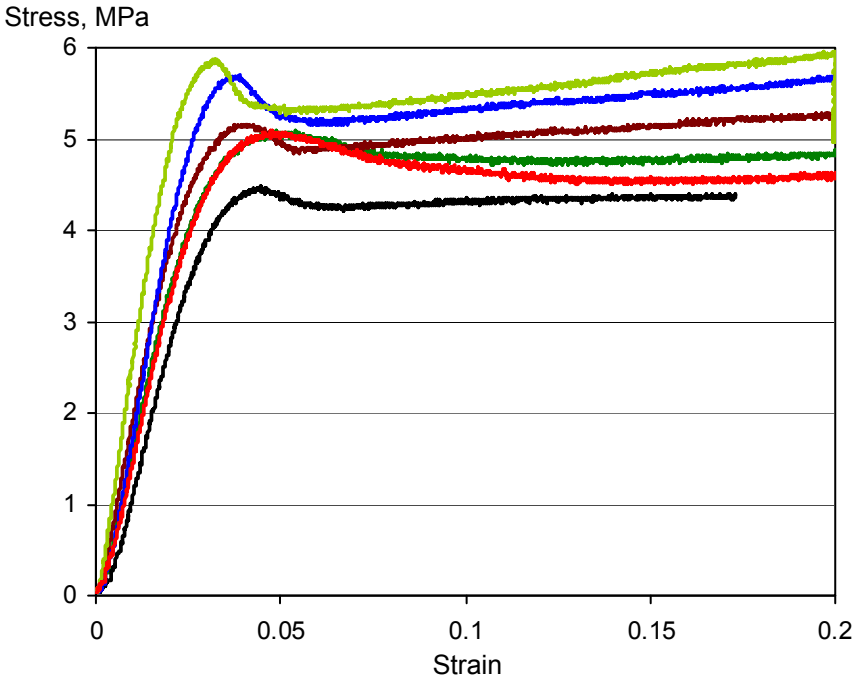

Figure 8. Compressive stress-strain curves of off-axis specimens for loading orientations of 0, 20, 45, 70, and 90 deg with the 1-2 plane.

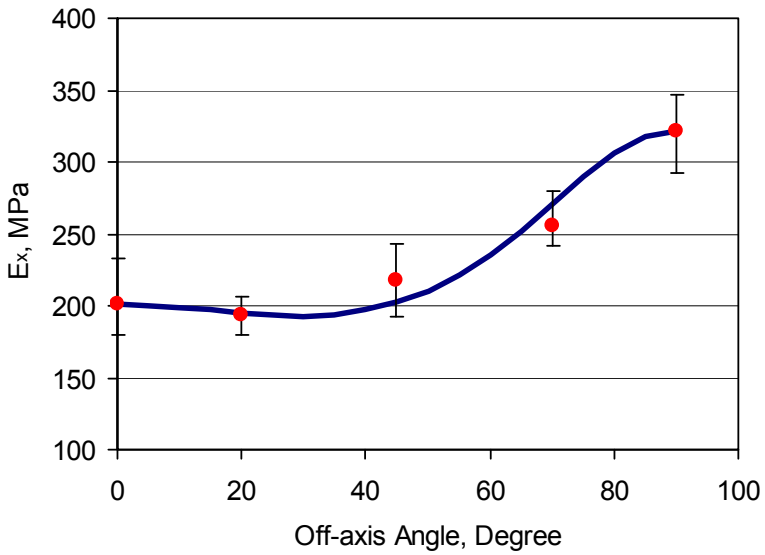

Figure 9. Variation of axial modulus with load orientation from the 1-2 plane

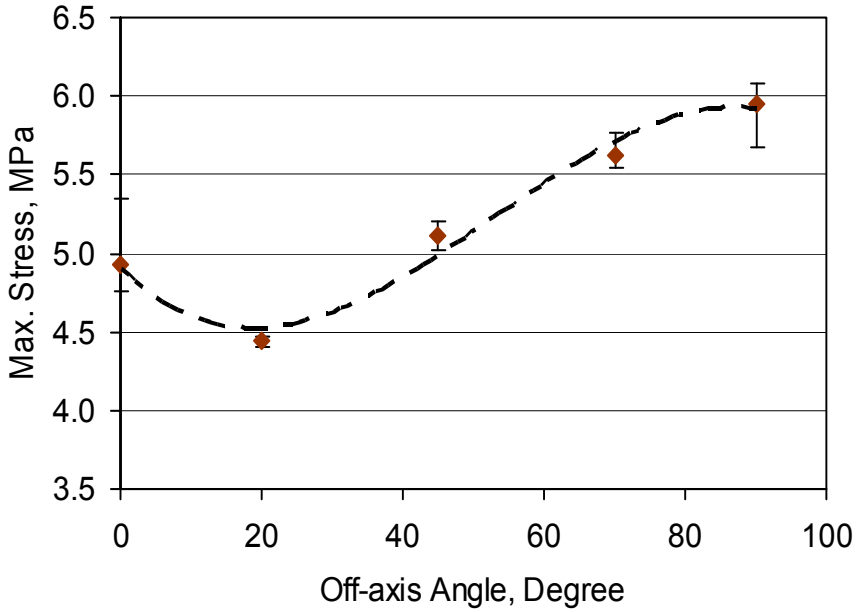

Figure 10. Variation of "critical stress" of cell structure with load orientation from the 1-2 plane

The above tests yielded the engineering constants, $E_1 = E_2$, E_3 , ν_{12} , $\nu_{13} = \nu_{23}$, G_{12} , $G_{13} = G_{23}$ of the material shown in Table 2.

Strain-Controlled Experiments

Compressive stress-strain curves along the in-plane and through-thickness directions for the strain-controlled (constrained) experiments are shown in Fig. 11. All strain components other than the one measured are constrained to be zero. These curves yield the stiffnesses $C_{11} = C_{22}$ and C_{33}.

$$\varepsilon_{ij} \cong 0 \qquad \varepsilon_{33} \neq 0$$

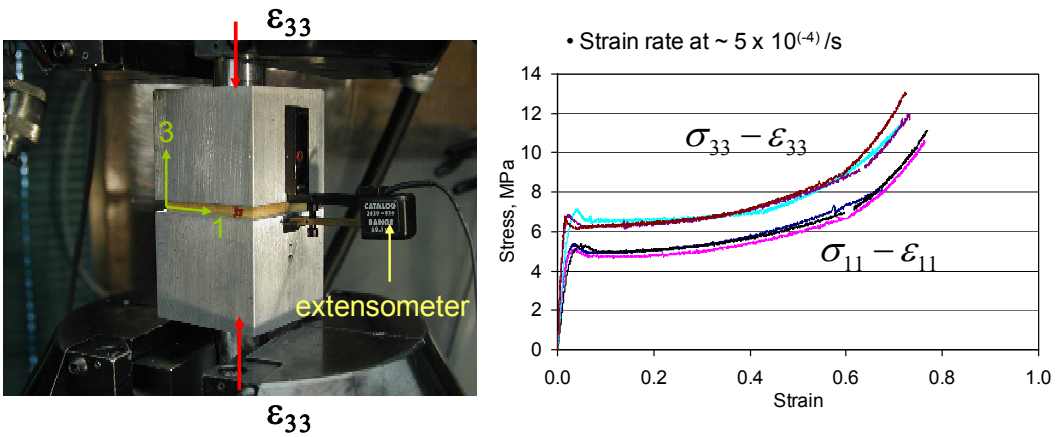

Figure 11. Stress-strain curves under uniaxial strain compression

Shear stress-strain curves are shown in Fig. 12. Only shear strain was applied, all other normal strains were zero. This test yields the shear moduli G_{12} and G_{13} .

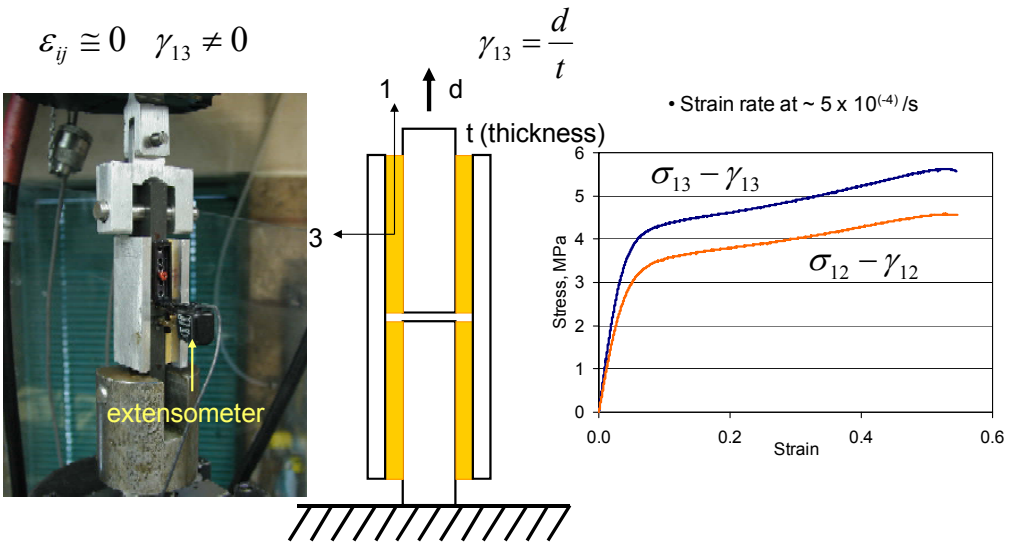

Figure 12. Strain-controlled shear stress-strain curves on the 1-2 and 1-3 planes.

Stress-strain curves under strain-controlled conditions were obtained at three strain rates and are shown in Fig. 13. Results at the highest rate of 10^3 s^{-1} were obtained with the SHPB system.

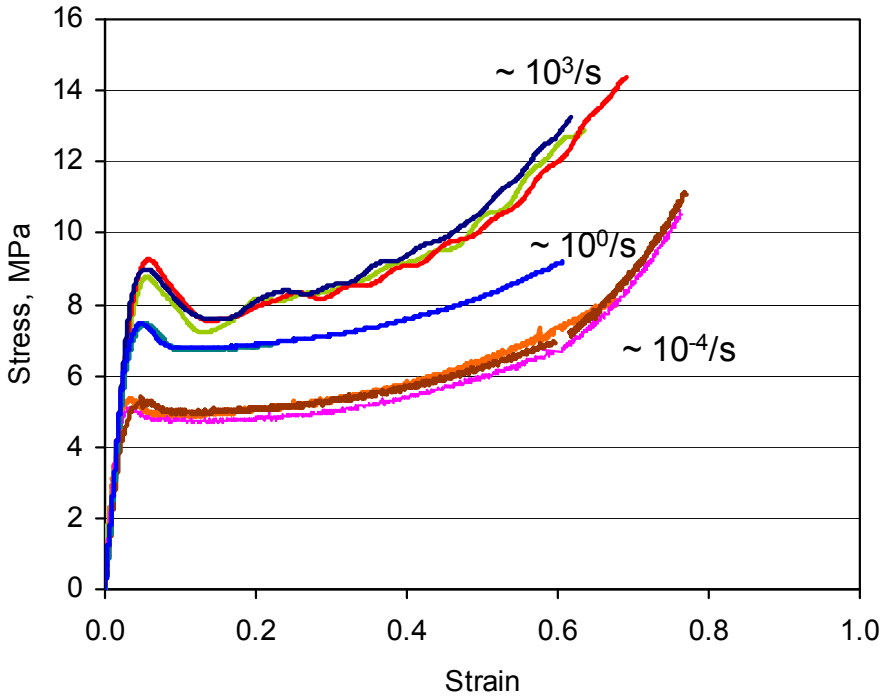

Figure 9. Compressive stress-strain curves in the in-plane (1 or 2) direction obtained under strain- controlled conditions.

The strain-controlled experiments did not yield the Poisson's ratios directly. These were calculated by the known interrelations between the engineering and mathematical stiffness constants.The mathematical constants $C_{11} = C_{22}$ and C_{33} are related to the engineering constants as follows:

$$C_{11} = \frac{E_1\left(E_1 - \nu_{13}^2 E_3\right)}{\left(E_1(1-\nu_{12}) - 2\nu_{13}^2 E_3\right)(1+\nu_{12})} \tag{1}$$

$$C_{33} = \frac{E_1 E_3 (1-\nu_{12})}{\left(E_1(1-\nu_{12}) - 2\nu_{13}^2 E_3\right)} \tag{2}$$

From the above, we can obtain the Poisson's ratios as follows:

$$\nu_{12} = \frac{-\frac{E_1}{E_3}\frac{C_{33}}{C_{11}}\left(1-\frac{E_3}{C_{33}}\right) \pm \sqrt{\left(\frac{E_1}{E_3}\frac{C_{33}}{C_{11}}\left(1-\frac{E_3}{C_{33}}\right)\right)^2 - 8\frac{E_1}{E_3}\frac{C_{33}}{C_{11}}\left(1+\frac{E_3}{C_{33}}\right)+16}}{4} \tag{3}$$

$$\nu_{13} = \sqrt{\frac{E_1(1-\nu_{12})}{2E_3}\left(1-\frac{E_3}{C_{33}}\right)} \tag{4}$$

Results from the second set of tests are summarized in Table 2 below.

Table 2. Mechanical Properties of Divinycell H250

Property	Strain Rate, s^{-1}		
	10^{-4}	1	10^{-3}
In-plane Young's Modulus $E_1 = E_2$, MPa	207		
Through-thickness Young's Modulus E_3, MPa	322		
Poisson's Ratio, ν_{12}	0.29	0.26	0.26
Poisson's Ratio, $\nu_{13} = \nu_{23}$	0.20	0.19	0.19
In-plane Shear Modulus, G_{12}, MPa	85	87	
Through-thickness Shear Modulus $G_{13} = G_{23}$, MPa	110	111	
Stiffness, $C_{11} = C_{22}$, MPa	250	247	254
Stiffness, C_{33}, MPa	388	378	399

Summary and Conclusions

An anisotropic cellular foam, Divinycell H250, used in sandwich structures was characterized under quasi-static and dynamic loading conditions. Two types of tests were conducted under quasi-static loading, stress-controlled and strain-controlled tests. Tests were run at various orientations with respect to the principal material axes. These tests allowed the determination of the complete set of both engineering and mathematical stiffness constants. Tests were also conducted at an intermediate strain rate of 1 s^{-1} and also at a high rate of 10^3 s^{-1} by means of a Split Hopkinson Pressure Bar. It was observed that the stiffness, based on the initial slope of the stress-strain curves, did not change with strain rate. However, the characteristic peak following the proportional limit increased noticeably with strain rate. This peak is the "critical point" corresponding to collapse initiation of the cells in the foam. This peak is followed by a "strain hardening" region before densification at very high strains.

Acknowledgement

The work described in this paper was sponsored by the Office of Naval Research (ONR). We are grateful to Dr. Y. D. S. Rajapakse of ONR for his encouragement and cooperation.

References

[1] Gibson, L.J. and M.F. Ashby, Cellular Solids. 2nd ed., New York: Cambridge University Press (1997).
[2] Daniel, I.M., E.E. Gdoutos, K.-A. Wang and J.L. Abot, "Failure Modes of Composite Sandwich Beams," International Journal of Damage Mechanics, **11**, 309-334 (2002).
[3] Gdoutos, E.E., I.M. Daniel, and K.A. Wang, "Failure of Cellular Foams under Multiaxial Loading," Composites Part A, **33**, 163-176, (2002).
[4] Flores-Johnson, E.A. and Q.A. Li, "Degradation of Elastic Modulus of Progressively Crushable Foams in Uniaxial Compression," Journal of Cellular Plastics, 44, 415-434, (2008).
[5] Abrate, S., "Criteria for Yielding or Failure of Cellular Materials," Journal of Sandwich Structures and Materials, **10**, 5-51, (2008).
[6] Ramon, O. and J. Mintz, "Prediction of Dynamic Properties of Plastic Foams from Constant Strain Rate Measurements," J. Appl. Polym. Scie., **40**(9-10),1683-1692 (1990).
[7] Daniel, I.M. and S. Rao, "Dynamic Mechanical Properties and Failure Mechanisms of PVC Foams," Dynamic Failure in Composite Materials and Structures, ASME Mechanical Engineering Congress and Exposition, AMD-Vol. **243**, 37-48 (2000).
[8] Viot, P., F. Beani and J.-L. Latallade,"Polymeric foam behavior under dynamic compressive loading," J. Mat. Scie., **40,** 5829-5837 (2005).
[9] Lee, Y.S., N.H. Park and H.S. Yoon, "Dynamic Mechanical Characteristics of Expanded Polypropylene Foams," J. Cellular Plastics, 46, 43-55 (2010).
[10] Zhang, Y., N. Kikuchi, V. Li, A. Yee and G. Nusholtz, "Constitutive Modeling of Polymeric Foam Material Subjected to Dynamic Crash Loading," International Journal of Impact Engineering, vol. 21, No. 5, pp. 369 386, 1998.
[11] Tagariellia, V.L., V.S. Deshpande, N.A. Fleck, and C. Chen, "A constitutive model for transversely isotropic foams, and its application to the indentation of balsa wood," International Journal of Mechanical Sciences, **47**, 666-686, (2005).
[12] Gielen, A.W.J., "A PVC-foam material model based on a thermodynamically elasto-plastic-damage framework exhibiting failure and crushing," International Journal of Solids and Structures, vol. 45, pp. 1896–1917, 2008.